arXiv:0711.0009v1 [quant-ph] 31 Oct 2007

Interference Between Competing Pathways in the Interaction of Three-Level Ladder Atoms and Radiation

Tony Y. Abi-Salloum
Physics Department, Drexel University, Philadelphia, Pennsylvania 19104, USA

(Dated: February 2, 2008, *Physical Review A*: To be resubmitted.)

In this paper we explore the physical origin of the transparency induced in absorbing three-level cascade atoms by the simultaneous interplay of two coherent beams of light. By utilizing the scattering technique we offer what we believe is a very convincing physical evidence for the existence, or for the absence, of quantum interference effects in the Autler-Townes (AT) and Electromagnetically Induced Transparency (EIT) phenomena.

I. INTRODUCTION

The interaction of two coherent fields with three-level atoms features a variety of phenomena which are at the forefront of research in field of non-linear optics today. A few examples of some effects include electromagnetically induced transparency [1], coherent population trapping [2], line narrowing and lasing without inversion [3]. In this article, we highlight first a number of optical phenomena of interest. Two of the reviewed phenomena are at the core of this study where quantum interference effects are investigated.

In 1990 the term “Electromagnetically Induced Transparency (EIT)” was introduced by Harris et al. [4] whose theoretical work showed an enhancement in the third-order susceptibility experienced by a probe field and simultaneously a decrease in the absorption of the same probe field in a collection of three-level atoms in a cascade configuration. Many reviews [1, 5, 6] have been written about EIT since its emergence. The first experiment confirming the EIT phenomenon was done in 1991 by Boller, Imamoglu, and Harris [7] in a Strontium lambda system. Boller and colleagues stated without proving that the transparency may be interpreted as a combination of the Stark effect and another interference phenomenon that may in turn be understood at the level of the dressed states.

In correspondence with the interpretation presented by Boller and his colleagues, the underlying physical phenomenon responsible for EIT has been generally assumed to be similar to the physical origin of the Fano profile [8]. In the Fano profile setting two ionization pathways, one direct and another one proceeding through an intermediate autoionized state, interfere leading to a zero transition probability and thus a reduction of the ionization probability.

Closely related to the EIT phenomenon but one that preceded EIT by almost 15 years, Coherent Population Trapping (CPT) [9, 10, 11, 12] is another important phenomenon that is featured by three-level atoms. While EIT is associated with the reduction in the absorption of the probe field due to the interference between different excitation pathways, CPT is characterized by the reduction in spontaneous emission due to the trapping of the population in the non-coupled state. Other important phenomena, such as Lasing Without Inversion (LWI) [3] and “subluminal” [13, 14, 15, 16, 17] and “superluminal” [18, 19] light, ‘slow’ and ‘fast’ light was also reviewed extensively in 2002 by Boyd [20], are consequences of the EIT and CPT effects.

A phenomenon which is quite unlike most of what we have surveyed this far in this paper is the so-called Autler-Townes (dynamic Stark-Shift) effect [21]. Even though, the AT effect resembles the EIT phenomenon in that they both reduce the absorption of a probe field at or near resonance, AT, studied by Cohen-Tannoudji [22], is generally not associated with interference. However, despite a large volume of literature devoted to the study of EIT and AT, nowhere has the manifestation of (or lack therefore) of interference in these two related systems been explicitly pointed out. This important difference between the two effects is the subject of investigation in this paper.

We begin our investigations by considering two cascade configurations. We denote the first cascade configuration (shown on the left in figure 1) as Cascade-EIT. This name, at least at this early point in this paper, recognizes the experiments [23, 24, 25] which showed EIT in this specific system. Switching the strengths of the fields leads to another cascade configuration which we denote as Cascade-AT (shown on the right in Fig. 1). At first, it may seem counter-intuitive that merely switching the strengths of the involved fields can dramatically affects the results. However, we stress that experiments show in the Cascade-EIT case [26] a reduction in absorption even when the coupling field is weak, while experiments show no similar features in the Cascade-AT case [27] in the same weak field regime. Cascade-EIT and Cascade-AT are the two configurations which we have selected for our in-depth analysis of the similarities and, specially, differences between the EIT and the AT effects.

Following Lounis and Cohen-Tannoudji [28] we interpret the absorption of a probe photon as a scattering process induced by the atom while interacting with several pump (coupling) photons. We calculate the corresponding scattering amplitude and, if they exist, we identify the multiple physical paths followed by the system as it evolves to its final state. The existence of compatible multiple paths in the transition amplitude results in quantum interference effects exhibited by the transition

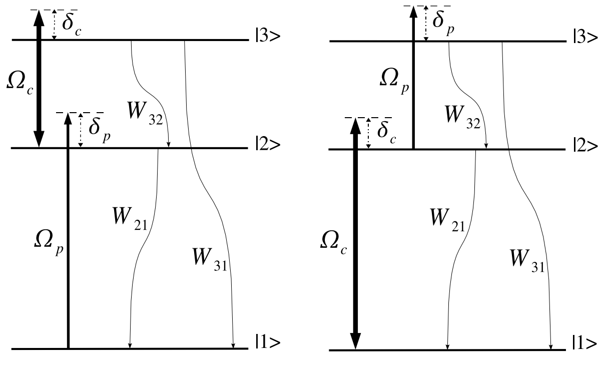

Cascade-EIT Cascade-AT

FIG. 1: Cascade-EIT and Cascade-AT configurations: Ω_c (Ω_p) and δ_c (δ_p) are the Rabi frequency and detuning of the coupling (probe) field. W_{ij} is the spontaneous decay rate from the level $|i\rangle$ to level $|j\rangle$.

probability. In 1993, Grynberg and Cohen-Tannoudji [29], using the same scattering technique [28], traced the physical origin of gain in the central resonance of the Mollow absorption spectrum. The scattering technique in the dressed states picture was also used to study the Vee system [3].

In the following section of this paper, two coupling field regimes are highlighted. Unlike the case in the strong coupling field regime where the two cascade systems display similar probe absorption spectra, in the weak field regime, which will be extensively studied in this paper, the two configurations present a critical difference. In section III, we survey the mathematical tools which are needed to calculate the probability that a system evolves from a given initial to a final state. For certain crucial technical reasons discussed in the introduction of section IV, only the Cascade-EIT configuration can be studied in the bare states picture. It is in this same section where we show the existence of two excitation-emission pathways in the process of absorption of a probe photon in the Cascade-EIT case. The results are clarified in the low saturation limit where we prove that the two pathways compete and interfere. Section V studies the scattering of a probe photon in the dressed states picture only in the low saturation limit due to physical requirements of the technique which will be discussed in the introduction of the section. Both configurations are studied. The expected absence of interfering pathways in the Cascade-AT case is verified. Also, the results found in the Cascade-EIT case are consistent with the ones found in the bare state picture.

II. MACROSCOPIC DIFFERENCES AND SIMILARITIES

The probe absorption spectrum (solid line in figure 2) of the Cascade-EIT configuration, which is proportional to the imaginary part of the density matrix element ρ_{21} [25],

$$\rho_{21} \;\propto\; -i\,\frac{\gamma_{13}-i(\delta_p+\delta_c)}{\frac{|\Omega_c|^2}{4}+[\gamma_{12}-i\delta_p][\gamma_{13}-i(\delta_p+\delta_c)]}, \tag{1}$$

and the probe absorption spectrum (dashed line in figure 2) of the Cascade-AT configuration, which is proportional to the imaginary part of ρ_{32} [30],

$$\rho_{32} \;\propto\; i\,\frac{\frac{|\Omega_c|^2}{4}}{\gamma_{12}^2+\delta_c^2+2\frac{|\Omega_c|^2}{4}} \;\times \tag{2}$$
$$\frac{\gamma_{23}+i\delta_p}{[\gamma_{13}+i(\delta_p+\delta_c)][\gamma_{23}+i\delta_p]+\frac{|\Omega_c|^2}{4}},$$

display similar features, mainly a reduction in absorption in the expected maximum absorptive probe field detuning range in the absence of the coupling field. Note that we changed several notations such as detunings, decay rates, density matrix elements, and Rabi frequencies, redefined the coupling Rabi frequency, included the spontaneous decay rate W_{31}, and also dropped multiplication factors for the sake of consistency between the two references [25, 30] and our work. All the previously used variables will be defined in the following sections when needed.

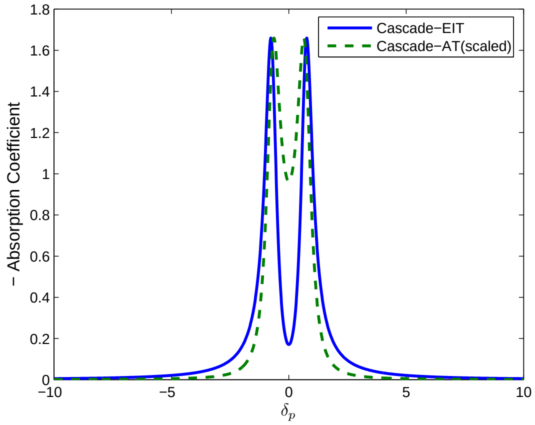

FIG. 2: Negative absorption coefficient of the probe field in the Cascade-EIT case (solid line) and Cascade-AT case (dashed line) function of the probe detuning. Theoretical values: γ_{12}=0.5, γ_{13}=0.105, γ_{23}=0.605, δ_c=0, Ω_c=1.5.

Figure 3 is a plot of the separation between the peaks of the absorption spectra at resonance ($\delta_c = 0$) function of the coupling field Rabi frequency. Monitoring the separation between the peaks reveals two regimes. The strong field regime ($\Omega_c \gg \gamma_{ij}$) has been studied by Cohen-Tannoudji [22, 31, 32] and co-authors. The authors study the absorption and fluorescence spectra of a variety of three-level systems using the dressed-atom approach [33] in the secular limit (the effective Rabi frequency of the system, which is related to the strengths of the different used fields, is much greater than the atomic decay rates) which in our case is equivalent to the strong coupling field regime. One of the common messages across the different studies presented by Cohen-Tannoudji and co-authors is that in the three-level system case and in the secular limit the absorption line of the probe field splits into two Lorentzian lines which at resonance are separated by the coupling field Rabi frequency. This split in the absorption line is a consequence of the AT effect [22] which at least in the secular limit is not associated with interference. Figure 3 displays the AT linear separation in the strong coupling field range of Rabi frequency.

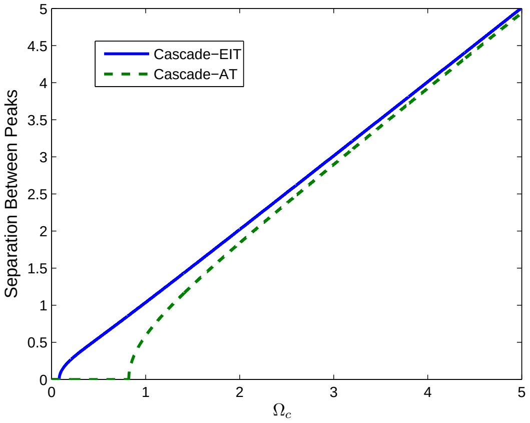

FIG. 3: Separation between the peaks of the probe absorption line in the Cascade-EIT case (solid line) and Cascade-AT case (dashed line) function of the coupling field Rabi frequency. Theoretical values: γ_{12}=0.5, γ_{13}=0.105, γ_{23}=0.605, δ_c=0.

The linear AT separation displayed by both cascade configurations shows that the AT effect dominates all other possibly existing phenomena in the strong coupling field regime. As the coupling field strength decreases it is obvious that in the Cascade-AT case the dip fills up quickly as the two Lorentzians start overlapping while in the Cascade-EIT case the transparency persists and the separation even goes above the linear line and does not vanish until the coupling field is almost turned off. This macroscopic evident difference between the two cascade configurations, which we believe is a manifestation of the microscopic difference between the two phenomena AT and EIT, is the point of investigation in this paper. For this very clear reason we focus in this work on the weak coupling field regime which could be achieved by either one of the two conditions $\Omega_c \ll \gamma_{ij}$ or $\Omega_c \ll \delta_c$ which are known as the low saturation limit. We note that the low saturation condition $\Omega_c \ll \gamma_{ij}$ varies between the different configurations and will be given later in the paper.

III. TECHNIQUE

In this section we provide an outline of the general elements of the scattering technique [32] that is adopted in this paper. The transition and probability amplitudes, which are related to the probability of absorption are defined and calculated non perturbatively in the first subsection III A and then rederived in the second subsection III B after the introduction of an operator called the Resolvent.

A. Transition and Probability Amplitudes

A system in an initial state $|i\rangle$ at a time t_i has a probability $\mathcal{P}_{fi}(t_f, t_i)$ of performing a transition to a final state $|f\rangle$ at a later time t_f. The system evolves between the two times, t_i and t_f, according to the unitary transformation

$$|f\rangle \;=\; U(t_f, t_i)|i\rangle, \tag{3}$$

where the evolution operator, $U(t_f, t_i)$, is defined as

$$U(t_f, t_i) \;=\; e^{-iH(t_f - t_i)/\hbar}, \tag{4}$$

and depends on the total Hamiltonian H.

The probability amplitude that the system will go from the initial state $|i\rangle$ to the final state $|f\rangle$ is defined as

$$\mathcal{S}_{fi} \;\equiv\; U_{fi} \;=\; \langle f|U(t_f, t_i)|i\rangle. \tag{5}$$

The transition probability, $\mathcal{P}$, is equal to the modulus squared of the the probability amplitude, $\mathcal{S}_{fi}$,

$$\mathcal{P}_{fi}(t_f, t_i) \;=\; |\mathcal{S}_{fi}|^2. \tag{6}$$

After substituting equation 3 into the Schrödinger equation for the final state we solve for the evolution operator, $U(t_f, t_i)$, which after a transformation into the interaction picture and a substitution into equation 5 leads to

$$\mathcal{S}_{fi} \;\simeq\; \delta_{fi} - 2\pi i \delta^{(T)}(E_f - E_i) \lim_{\eta \to 0_+} \mathcal{T}_{fi}, \tag{7}$$

where we defined the transition amplitude, $\mathcal{T}_{fi}$ (not to be confused with the probability amplitude $\mathcal{S}_{fi}$), as

$$\mathcal{T}_{fi} \;=\; \langle f|V|i\rangle + \langle f|V \frac{1}{E_i + i\eta - H} V|i\rangle, \tag{8}$$

V being the interaction part of the Hamiltonian, η being a positive real number introduced by the identity

$$e^{iE(t_2 - t_1)/\hbar}\Theta(t_2 - t_1) \;=\; \lim_{\eta \to 0_+} -\frac{1}{2\pi i} \int_{-\infty}^{+\infty} \frac{e^{-iE(t_2 - t_1)/\hbar}}{E + i\eta - E_k} dE, \tag{9}$$

where $\Theta(t_2 - t_1)$ is the Heaviside function. We also used in equation 7 the diffraction function $\delta^{(T)}(E_f - E_i)$, which is defined as

$$\delta^{(T)}(E_f - E_i) \;=\; \frac{1}{\pi} \frac{\sin\left[(E_f - E_i)T/2\hbar\right]}{E_f - E_i}, \tag{10}$$

where T is the duration of the interaction.

B. Resolvent Operator

We introduce the resolvent operator of the total Hamiltonian, H, in the form

$$G(z) \ = \ \frac{1}{z-H}, \tag{11}$$

and reduce equation 8 to

$$\mathcal{T}_{fi} \ = \ \langle f|V|i\rangle + \langle f|VG(E_i+i\eta)V|i\rangle. \tag{12}$$

For use later on, we can re-write equation 12 by introducing the identity operator $\hat{1} \equiv \sum_k |k\rangle\langle k|$, so that

$$\begin{aligned} \mathcal{T}_{fi} \ &= \ \langle f|V|i\rangle + \langle f|V\hat{1}\frac{1}{E_i+i\eta-H}\hat{1}V|i\rangle, & (13)\\ &= \ \langle f|V|i\rangle + \sum_k\sum_l V_{fk}V_{li}\langle k|G(E_i+i\eta)|l\rangle. & (14)\end{aligned}$$

In the cases of interest where $|f\rangle \neq |i\rangle$ the probability $\mathcal{P}_{fi}$ (Eq. 6) is given by

$$\mathcal{P}_{fi} \ = \ 4\pi^2\left[\delta^{(T)}(E_f-E_i)\right]^2 \ |\lim_{\eta\to 0_+}\mathcal{T}_{fi}|^2, \tag{15}$$

which implies that

$$\begin{aligned}\mathcal{P}_{fi} \ &= \ \pi^2\left[\delta^{(T)}(E_f-E_i)\right]^2 \times \\ &\quad |V_{fi} + \sum_{k,l}V_{fk}V_{li}\langle k|\lim_{\eta\to 0_+}G(E_i+i\eta)|l\rangle|^2. \quad (16)\end{aligned}$$

The states $|k\rangle$ and $|l\rangle$ are discrete intermediate states of the scattering process between the initial and final states, $|i\rangle$ and $|f\rangle$. The system is not observed at the intermediate states, but the the probability amplitude between the initial and final states is the sum over all probability amplitudes of all the intermediate states.

The matrix element $\langle k|G(E_i+i\eta)|l\rangle$ of the resolvent operator, G, is the matrix element of G projected onto the two subspaces to which the states $|k\rangle$ and $|l\rangle$ belong. For example, if the two intermediate states $|k\rangle$ and $|l\rangle$ belong to the same subspace $\mathcal{E}_o$ which is made of the set of quasi-degenerate and coupled states $\{|\varphi_1\rangle, \ldots, |\varphi_n\rangle\}$, we have

$$G_{kl}(E_i+i\eta) = \langle k|PG(E_i+i\eta)P|l\rangle, \tag{17}$$

where the projector P is defined as

$$P \ = \ \sum_i^n |\varphi_i\rangle\langle\varphi_i|. \tag{18}$$

The other possible case is when only one of the intermediate states, $|l\rangle$ for example, belongs to the subspace $\mathcal{E}_o$ while the second state, $|k\rangle$, belongs to the supplementary subspace of $\mathcal{E}_o$, $\mathcal{L}_o$. In this case we have

$$G_{kl}(E_i+i\eta) = \langle k|QG(E_i+i\eta)P|l\rangle, \tag{19}$$

where Q is the supplementary projector of P defined as

$$Q \ = \ \hat{1} - P. \tag{20}$$

After some calculations we find that

$$\begin{aligned} PG(z)P \ &= \ \frac{P}{z-PH_oP-PR(z)P}, & (21)\\ QG(z)P \ &= \ \frac{Q}{z-QHQ}\,V\,PG(z)P. & (22)\end{aligned}$$

where H_o is the unperturbed Hamiltonian, H is the total Hamiltonian ($H = H_o + V$), and R(z) is the level shift operator defined as

$$R(z) \ = \ V + V\frac{Q}{z-QHQ}V. \tag{23}$$

IV. BARE STATES PICTURE

The probability that a system will evolve from an initial to a final state is independent of the picture in which the calculations are carried out. The different pictures only effect the intermediate states associated with the pathways followed by the system as it evolves from the initial to the final state. Some pictures, the dressed states picture for example, pose specific restrictions to the application of the scattering technique. This fact will be addressed further in section V where the dressed states picture will be used.

In this section we adopt the bare states picture seeking an understanding of the possible pathways followed by the atom through intermediate bare states in the process of scattering one probe photon. We consider the physically realistic situation where the system, in this case the bare atom, is initially in a quasi-stable state. At the end of the scattering process the system must also exist in a quasi-stable state. If this was not the case, the evolution would not yet be over. In this section as in the subsequent sections, we will always only consider initial and final states that are quasi-stable.

In a cascade system the excited atomic states $|2\rangle$ and $|3\rangle$ are not stable because of their spontaneous decay out of these states. This leaves the ground state, $|1\rangle$, as the only bare atomic state which can be used as an initial and final state for the scattering process. In the Cascade-EIT configuration, unlike the Cascade-AT configuration, the state $|1\rangle$ is coupled by a weak field (probe) to state $|2\rangle$. This fact keeps the state $|1\rangle$ stable. This situation is quite different from the Cascade-AT case where state $|1\rangle$ is coupled to state $|2\rangle$ by a strong field (coupling). The fact that the strong coupling field forces the atom to oscillate between the two states $|1\rangle$ and $|2\rangle$ with a large Rabi frequency makes the state $|1\rangle$ unstable. The problem of not having a bare stable state in the Cascade-AT configuration eliminates the possibility of applying the scattering technique to this configuration in the bare states picture. We study in this section only the Cascade-EIT configuration. In the next section, instead, we show that one of the dressed states in either configuration is quasi-stable and this allows the study of the Cascade-AT configuration in the dressed state picture.

The initial setting of the Cascade-EIT system of interest involves the atom in the atomic ground state $|1\rangle$ interacting simultaneously with the coupling field, having N_c photons in its mode, one probe photon, and zero photons in all the different vacuum modes, which we label by a subindex j. Thus, the initial state has the form

$$|i\rangle \; = \; |1;(1)_p,(N_c)_c,(0)_j\rangle. \tag{24}$$

Considering only one photon in the probe field corresponds to the simplest scattering process, where one probe photon is absorbed followed at a later time by the emission of a new photon in one of the vacuum modes. We did examine the case where N_P ($N_P > 1$) photons exist in the probe field. We found that the inclusion of more than one probe photon is associated with higher order interactions which is out of the scope of this paper because of their low orders of magnitudes.

Based on the scattering process and the requirement that the state be quasi stable, the final state corresponds to the situation where the atom is in its ground state with N_c photons in the coupling field, no photons in the probe field, and one photon of frequency ω in the corresponding vacuum mode (with all other vacuum modes having zero photons). This state is given by

$$|f\rangle \; = \; |1;(0)_p,(N_c)_c,(1)_\omega\rangle. \tag{25}$$

After using the appropriate initial (Eq. 24) and final (Eq. 25) sates, the transition amplitude, $\mathcal{T}_{fi}$ (Eq. 12), reduces to

$$\mathcal{T}_{fi} \; = \; \frac{\hbar^2\Omega\Omega_p}{4}\langle\varphi_2|G(E_i+i\eta)|\varphi_2\rangle, \tag{26}$$

where Ω_p and Ω are respectively the Rabi frequencies of the probe and the non-zero vacuum field defined in this case as

$$\Omega_p \; = \; -2\mu_{12}\sqrt{\frac{\hbar\omega_p}{2\epsilon_o L^3}}, \tag{27a}$$

$$\Omega \; = \; -2\mu_{12}\sqrt{\frac{\hbar\omega}{2\epsilon_o L^3}}, \tag{27b}$$

where L^3 is equal to the volume of the cavity, and where the discrete state $|\varphi_2\rangle$ is defined as

$$|\varphi_2\rangle \; = \; |2;(0)_p,(N_c)_c,(0)_j\rangle. \tag{28}$$

By setting the energy of the state $|\varphi_2\rangle$ as the energy reference, $E_{\varphi_2}=0$, and after defining the state $|\varphi_3\rangle$ as

$$|\varphi_3\rangle \; = \; |3;(0)_p,(N_c-1)_c,(0)_j\rangle, \tag{29}$$

we find that the states $|i\rangle$ and $|\varphi_3\rangle$ have the energies

$$E_i \; = \; \hbar\delta_p, \tag{30a}$$

$$E_{\varphi_3} \; = \; -\hbar\delta_c, \tag{30b}$$

where $\delta_p=\omega_p-\omega_{12}$ and $\delta_c=\omega_c-\omega_{23}$, and are quasi-degenerate with the state $|\varphi_2\rangle$ (the quasi-degenerate results from the smallness of the detuning parameters relative to all the other frequencies of the problem).

In the infinite volume limit, $L\to\infty$, we find that the coupling between the states $|\varphi_3\rangle$ and $|\varphi_2\rangle$,

$$\langle\varphi_2|V|\varphi_3\rangle \; = \; \hbar\frac{\Omega_c}{2} \overset{L\to\infty}{\not\longrightarrow} 0, \tag{31}$$

where Ω_c is the Rabi frequency of the coupling field defined as $\Omega_c = -2\mu_{23}\sqrt{\frac{\hbar\omega_c N_c}{2\epsilon_o L^3}}$, remains finite.

Unlike the coupling between the states $|\varphi_3\rangle$ and $|\varphi_2\rangle$, the coupling between the two states $|\varphi_2\rangle$ and $|i\rangle$,

$$\langle\varphi_2|V|i\rangle \; = \; \hbar\frac{\Omega_p}{2} \xrightarrow{L\to\infty} 0, \tag{32}$$

vanishes in the infinite volume limit. This fact eliminates the initial state $|i\rangle$ from the subspace of the state $|\varphi_2\rangle$.

In this case the matrix element $\langle\varphi_2|G(E_i+i\eta)|\varphi_2\rangle$ is the element of the operator G projected onto the subspace $\mathcal{E}_o$ defined as

$$\mathcal{E}_o = \{|\varphi_2\rangle,|\varphi_3\rangle\}\,. \tag{33}$$

Using equation 21, the projection of the resolvent operator, $G(E_i+i\eta)$, into the subspace $\mathcal{E}_o$, leads to

$$\lim_{\eta\to 0_+} PG(E_i+i\eta)P \; = \; \frac{\hbar}{D}\begin{pmatrix} \delta_p+iW_{21}/2 & -\Omega_c/2 \\ -\Omega_c/2 & \delta_p+\delta_c+i(W_{32}+W_{31})/2 \end{pmatrix}, \tag{34}$$

where D is the determinant of the matrix $(PGP)^{-1}$ and is given by

$$D \; = \; \hbar^2\left(\delta_p+\delta_c+i\gamma_{13}\right)\left(\delta_p+i\gamma_{12}\right)-\hbar^2\frac{\Omega_c^2}{4}, \tag{35}$$

where W_{ij} is the spontaneous decay rate from level i to level j (i,j=2,3) and γ_{ij} is the corresponding polarization decay rate, which in free space is given by

$$\gamma_{ij} = \sum_{k=1}^{3}\left(W_{ik}+W_{jk}\right). \tag{36}$$

A. Resonances

The determinant D (Eq. 35) can be written explicitly in terms of the eigenvalues of the matrix $(PGP)^{-1}$, i.e.

$$D = \hbar^2(\delta_p - Z_{II})(\delta_p - Z_{III}), \tag{37}$$

where the eigenvalue, Z_{II} and Z_{III} are given by

$$2Z_{II} \; = \; -(\delta_c+i\gamma_{23})+\sqrt{(\delta_c+i\gamma_{13}-i\gamma_{12})^2+\Omega_c^2}, \tag{38a}$$

$$2Z_{III} \; = \; -(\delta_c+i\gamma_{23})-\sqrt{(\delta_c+i\gamma_{13}-i\gamma_{12})^2+\Omega_c^2}. \tag{38b}$$

After writing the transition amplitude (Eq. 26) in terms of the eigenvalues we obtain

$$\mathcal{T}_{fi} = \frac{\hbar\Omega\Omega_p}{4(Z_{II}-Z_{III})}\times \left(\frac{Z_{II}+\delta_c+i\gamma_{13}}{\delta_p-Z_{II}} - \frac{Z_{III}+\delta_c+i\gamma_{13}}{\delta_p-Z_{III}}\right). \quad (39)$$

Because the transition amplitude is the sum of two complex numbers, the scattering process may be characterized by an interference between two possible evolution pathways followed by the atom during the scattering process. Each of the two complex numbers is associated with an intermediate state, or a sequence of intermediate states. We denote these pathways as first and second resonance and, thus, write equation 39 in the form

$$\mathcal{T}_{fi} = 1^{\text{st}}\text{ Resonance} + 2^{\text{nd}}\text{ Resonance}. \quad (40)$$

We note here that what is as important as the existence of two resonances is the relative order of magnitude between the amplitudes of these resonances. This business of relative orders will be clarified in the next subsection in the low saturation limit where the interference effect is significant.

When the coupling field is turned off, $\Omega_c = 0$, the eigenvalues, Z_{II} and Z_{III}, approach their unperturbed values

$$Z_{II} \rightarrow -i\gamma_{12}, \quad (41a)$$

$$Z_{III} \rightarrow -\delta_c - i\gamma_{13}. \quad (41b)$$

Consistently, we expect that the eigenstates $|\bar{\varphi}_2\rangle$ and $|\bar{\varphi}_3\rangle$ which correspond to the eigenvalues Z_{II} and Z_{III} approach the unperturbed states $|\varphi_2\rangle$ and $|\varphi_3\rangle$ in the absence of the coupling field ($\Omega_c = 0$). Note that the bars in $|\bar{\varphi}_2\rangle$ and $|\bar{\varphi}_3\rangle$ are added to distinguish the eigenstates from their corresponding unperturbed states $|\varphi_2\rangle$ and $|\varphi_3\rangle$.

Based on the understanding of equation 41a we set the eigenvalue Z_{II} in the form

$$Z_{II} = -i\gamma_{12} - \delta_c' + i\gamma_c', \quad (42)$$

where δ_c' and γ', which will be derived later on in this paper, are correction terms which are consequences of the presence of the coupling field. In addition, after using the conservation of the trace we obtain

$$Z_{III} = -\delta_c - i\gamma_{13} + \delta_c' - i\gamma_c'. \quad (43)$$

The corrections to the energy and radiative broadening of levels $|2\rangle$ and $|3\rangle$ due to the existence of the coupling field can be understood in the following way. The term $-\delta_c'$ (δ_c') represents the light shift of level $|2\rangle$ ($|3\rangle$). Similarly, the term -γ_c' (γ_c') is the radiative correction of the unperturbed level $|2\rangle$ ($|3\rangle$).

The first resonance is centered at $\delta_p = \Re(Z_{II}) = -\delta_c'$, which implies that $\hbar\omega_p = \hbar\omega_{21} - \hbar\delta_c'$, which is the optical resonance between level $|1\rangle$ and the shifted level $|2\rangle$. This optical resonance has a width of $\gamma_{12} - \gamma_c'$ which approaches γ_{12} when Ω_c tends to zero.

The second resonance is centered at $\delta_p = \Re(Z_{III}) = -\delta_c + \delta_c'$ which is equivalent to $\hbar\omega_p + \hbar\omega_c = \hbar\omega_{31} + \hbar\delta_c'$. This resonance corresponds to the Raman resonance condition between the light-shifted level $|3\rangle$ and level $|1\rangle$ and has a linewidth of $\gamma_{13} + \gamma_c'$.

B. Low Saturation Limit

In this section we consider the low saturation limit in which the interference effect is not dominated by any other phenomena such as the AT one. In this case the level shifts and the linewidths corrections acquire more transparent forms and the pathways corresponding to the different resonances become obvious.

In the low saturation limit, $\Omega_c^2/(\gamma_{12}-\gamma_{13})^2 \ll 1$ or $\Omega_c^2/\delta_c^2 \ll 1$, equation 38b reduces to

$$Z_{III} = -\delta_c - i\gamma_{13} - \frac{\Omega_c^2/4}{\delta_c + i(\gamma_{13}-\gamma_{12})}, \quad (44)$$

which after comparison with equation 43 leads to

$$\delta_c' = -\delta_c \frac{\Omega_c^2/4}{\delta_c^2 + (\gamma_{13}-\gamma_{12})^2}, \quad (45a)$$

$$\gamma_c' = -(\gamma_{13}-\gamma_{12}) \frac{\Omega_c^2/4}{\delta_c^2 + (\gamma_{13}-\gamma_{12})^2}. \quad (45b)$$

In the low saturation limit the transition amplitude (Eq. 39) takes the form

$$\mathcal{T}_{fi} = \frac{\hbar\Omega\Omega_p}{4}\left(\frac{1}{\delta_p - Z_{II}} + \left[\frac{-\Omega_c/2}{\delta_c + i(\gamma_{13}-\gamma_{12})}\right]^2 \frac{1}{\delta_p - Z_{III}}\right), \quad (46)$$

where the two terms between the parentheses correspond to the first and second resonances.

The first resonance is given explicitly by

$$1^{\text{st}}\text{ Resonance} = \frac{\hbar\Omega\Omega_{\text{p}}}{4}\frac{1}{\delta_{\text{p}} + \delta_c' + \text{i}(\gamma_{12}-\gamma_c')}, \quad (47)$$

where $\gamma_c' << \gamma_{12}$. We also consider the limit $\delta_c' << \delta_p$ which yields the final result

$$1^{\text{st}}\text{ Resonance} \approx \frac{\hbar\Omega}{2}\,\frac{1}{\hbar(\delta_{\text{p}} + \text{i}\gamma_{12})}\,\frac{\hbar\Omega_{\text{p}}}{2}. \quad (48)$$

The first resonance is the product of three factors. Starting from the right hand side, the factor $\hbar\Omega_p/2$ describes the absorption process of the probe photon. This absorption process leaves the atom in the state 2 which has an energy $\hbar\delta_p$ and a radiative decay γ_{12}. The last factor of the first resonance, $\hbar\Omega/2$, is associated with the emission of a photon of frequency ω into one of the vacuum modes. Thus, the pathway of the scattering process corresponding to the first resonance can be sketched

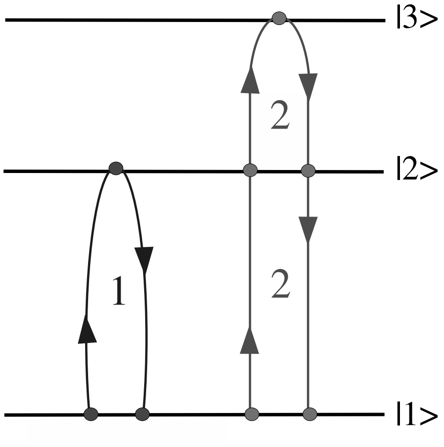

FIG. 4: Resonances of the Cascade-EIT configuration in the bare states picture.

graphically as shown in figure 4. We also note for later discussion at the end of this subsection that the first resonance is of zeroth order in the coupling field, Ω_c.

The second resonance has the form

$$\begin{aligned} 2^{\text{nt}}\text{ Resonance } &= \frac{\hbar\Omega\Omega_p}{4}\left[\frac{-\Omega_c/2}{\delta_c + i(\gamma_{13}-\gamma_{12})}\right]^2 \times \\ & \frac{1}{\delta_p+\delta_c-\delta_c'+i(\gamma_{13}+\gamma_c')}. \end{aligned} \tag{49}$$

This contribution becomes especially large when $\delta_p \approx -\delta_c + \delta_c'$ leading to the approximation $\delta_c \approx -\delta_p + \delta_c' \approx -\delta_p$. In this case, equation 49 reduces to

$$\begin{aligned} 2^{\text{nd}}\text{ Resonance } &\approx \frac{\hbar\Omega}{2}\frac{1}{\hbar(\delta_p + i(\gamma_{12}-\gamma_{13}))}\times \\ & \frac{\hbar\Omega_c}{2}\frac{1}{\hbar(\delta_p+\delta_c-\delta_c'+i(\gamma_{13}+\gamma_c'))}\frac{\hbar\Omega_c}{2}\times \\ & \frac{1}{\hbar(\delta_p + i(\gamma_{12}-\gamma_{13}))}\frac{\hbar\Omega_p}{2}. \end{aligned} \tag{50}$$

The second resonance (Fig. 4) corresponds to the absorption of the probe photon followed by simultaneous absorption and emission of coupling field photons and ending with the spontaneous emission of one vacuum photon.

The transition amplitude (Eq. 46), after all the approximations discussed previously, reduces to

$$\begin{aligned} \mathcal{T}_{fi} &\approx \frac{\hbar\Omega}{2}\frac{1}{\hbar(\delta_p+i\gamma_{12})}\frac{\hbar\Omega_p}{2} + \frac{\hbar\Omega}{2}\frac{1}{\hbar(\delta_p + i(\gamma_{12}-\gamma_{13}))}\times \\ & \frac{\hbar\Omega_c}{2}\frac{1}{\hbar(\delta_p+\delta_c-\delta_c'+i(\gamma_{13}+\gamma_c')))}\frac{\hbar\Omega_c}{2}\times \\ & \frac{1}{\hbar(\delta_p + i(\gamma_{12}-\gamma_{13}))}\frac{\hbar\Omega_p}{2}. \end{aligned} \tag{51}$$

We stress again the fact that the requirement to have interference is not only the existence of two or more interfering pathways but also comparable probability amplitudes between the resonances. In the Cascade-EIT case, the second resonance (Eq. 50) approaches the first resonance (Eq. 48) in magnitude as Ω_c becomes larger than γ_{13}, a situation which does not violate the low saturation condition, $\Omega_c^2/(\gamma_{12}-\gamma_{13})^2 \ll 1$.

V. DRESSED STATES PICTURE

Earlier, we mentioned that quasistable bare states do not exist in the Cascade-AT configuration. This makes the scattering technique unsuitable for the analysis of the scattering process. This difficulty can be removed in the dressed states picture, and in particular in the low saturation limit, as we are going to show in this section.

As our first step we describe the Cascade-AT configuration in the dressed states picture and prove the absence of interference in the low saturation limit. In subsection V B we study the Cascade-EIT case and reproduce the results found in the bare state picture (the two pictures, of course, must be equivalent to each other).

A. Cascade-AT

In the low saturation limit, $\Omega_c^2/\delta_c^2 \ll 1$, the two eigenstates of the interaction Hamiltonian of the Cascade-AT system have the form

$$|a(N_c)\rangle = |1,N_c\rangle + \frac{\Omega_c}{2\delta_c}|2,N_c-1\rangle, \tag{52a}$$

$$|b(N_c)\rangle = |2,N_c-1\rangle - \frac{\Omega_c}{2\delta_c}|1,N_c\rangle, \tag{52b}$$

where $\delta_c = \omega_c - \omega_{12}$ and the coupling Rabi frequency is defined as

$$\Omega_c = -2\mu_{12}\sqrt{\frac{\hbar\omega_c N_c}{2\epsilon_o L^3}}, \tag{53}$$

and correspondingly the eigenvalues of the eigenstates (Eqs. 52) are given by

$$E_a = 0, \tag{54a}$$

$$E_b = -\delta_c. \tag{54b}$$

The dressed state $|a(N_c)\rangle$ (Eq. 52a) is made of the sum of the atomic bare state $|1\rangle$ and a correction term due to the coupling of the atom with the field. Because the correction term is small in the low saturation limit, the spontaneous decay rate out of level $|a(N_c)\rangle$ is approximately equal to that of the ground state, $|1\rangle$, i.e. the state is quasi-stable.

The same argument holds for the other dressed state, $|b(N_c)\rangle$, which approaches to the atomic state $|2\rangle$ in the absence of the coupling field. Based on the previous arguments the total decay rates of the two dressed states are given by

$$\Gamma_a = 0, \tag{55a}$$

$$\Gamma_b = W_{21}. \tag{55b}$$

In this case the dressed state $|a(N_c)\rangle$ is quasi-stable and can be used as the initial and final state of the scattering process. The process begins with one photon in the probe field and ends with one photon of energy $\hbar\omega'$ in the vacuum and no photons in the probe field. Thus, we define the following initial and final states

$$|i\rangle \;=\; |a(N_c),(1)_p,(0)_j\rangle, \qquad (56a)$$
$$|f\rangle \;=\; |a(N_c),(0)_p,(1)_{\omega'}\rangle. \qquad (56b)$$

In this case the transition amplitude (Eq. 12) reduces to

$$T_{fi}(E_i+i\eta) = \frac{\hbar^2\Omega'\Omega_p}{4}\left(\frac{\Omega_c}{2\delta_c}\right)^2 G_{33}(E_i+i\eta), \qquad (57)$$

where we defined the Resolvent matrix element $G_{33}(E_i+i\eta)$ as

$$\begin{aligned} G_{33}(E_i+i\eta) \;=\; & \langle 3(N_c),(0)_p,(0)_j| \times \\ & G(E_i+i\eta)|3(N_c),(0)_p,(0)_j\rangle, \end{aligned} \qquad (58)$$

and the probe and non-zero vacuum field Rabi frequencies as

$$\Omega' \;=\; -2\mu_{23}\sqrt{\frac{\hbar\omega'}{2\epsilon_o L^3}}, \qquad (59a)$$
$$\Omega_p \;=\; -2\mu_{23}\sqrt{\frac{\hbar\omega_p}{2\epsilon_o L^3}}. \qquad (59b)$$

The intermediate state $|3(N_c),(0)_p,(0)_j\rangle$ belongs to its own one dimensional space. In this case, the corresponding form of equation 21 in a one dimensional space leads to

$$G_{33}(E_i+i\eta) \;=\; \frac{1}{E_i+i\eta-E_3-R_{33}}. \qquad (60)$$

where the matrix element R_{33} of the level-shift operator is given by

$$\lim_{\eta\to 0_+} R_{33}(E_i+i\eta) \;=\; -i\hbar\frac{W_{32}+W_{31}}{2}, \qquad (61)$$

and E_i (E_3) is the energy of the state $|i\rangle$ ($|3(N_c),(0)_p,(0)_j\rangle$), $E_i - E_3 = \hbar(\delta_p+\delta_c)$, where in the Cascade-AT case the probe detuning, δ_p, is defined as $\delta_p = \omega_p - \omega_{23}$.

After substituting equation 60 into equation 57 we obtain

$$T_{fi}(E_i+i\eta) \;=\; \frac{\Omega_c}{2\delta_c}\frac{\hbar\Omega'}{2}\frac{1}{\hbar\left(\delta_p+\delta_c+i\gamma_{13}\right)}\frac{\hbar\Omega_p}{2}\frac{\Omega_c}{2\delta_c}, \qquad (62)$$

where we replaced $(W_{32}+W_{31})/2$ with the polarization decay rate γ_{13}, which can be obtained from equation 36.

The transition amplitude (Eq. 62) consists of only one term corresponding to a single resonance. There is only one complex number associated with the only pathway followed by the dressed atom as it evolves from the initial state (Eq. 56a) to the final state (Eq. 56b). This fact shows the absence of interference in the absorption process of a probe photon in the Cascade-AT case in the weak coupling field regime. The process described by this transition amplitude is shown by figure 5 where we have taken the detuning of the coupling field to be negative, a choice which leads to a higher energy level for the state $|b(N_c)\rangle$, relative to the state $|a(N_c)\rangle$. In addition to the stimulated absorption and emission of photons out and into the mode of the coupling field within the dressed state $|a(N_c)\rangle$, the scattering process involves the absorption of a probe photon followed by the emission of a photon in the vacuum field via the intermediate state $|3(N_c),(0)_p,(0)_j\rangle$. It is true that other pathways of higher order of interaction in the coupling field exist but these processes are extremely weak and can be ignored in the low saturation limit. We did beside the work presented in this paper extensively check out the first higher order process at resonance, $\delta_c = 0$, and proved that it can indeed be ignored in the low saturation limit $\Omega_c^2/\gamma_{12}^2 \ll 1$.

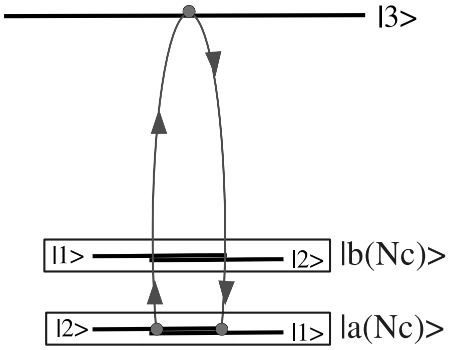

FIG. 5: Resonances of the Cascade-AT configuration in the dressed states picture.

B. Cascade-EIT

The dressed states of the Cascade-EIT system are

$$|a(N_c)\rangle \;=\; |2,N_c\rangle + \frac{\Omega_c}{2\delta_c}|3,N_c-1\rangle, \qquad (63a)$$
$$|b(N_c)\rangle \;=\; |3,N_c-1\rangle - \frac{\Omega_c}{2\delta_c}|2,N_c\rangle. \qquad (63b)$$

We use here the same initial and final states (Eqs. 24 and 25) defined in the bare states picture. In the low saturation limit, $\Omega_c^2/\delta_c^2 \ll 1$, and in the dressed states picture the transition amplitude (Eq. 12) reduces to

$$\begin{aligned} \mathcal{T}_{fi} &= \frac{\hbar^2\Omega\Omega_p}{4} \times \\ & [\langle a(N_c);(0)_p,(0)_j|G(E_i+i\eta)|a(N_c);(0)_p,(0)_j\rangle + \\ & \frac{\Omega_c^2}{4\delta_c^2}\langle b(N_c);(0)_p,(0)_j|G(E_i+i\eta)|b(N_c);(0)_p,(0)_j\rangle]. \end{aligned} \tag{64}$$

The Resolvent matrix elements corresponding to the intermediate states $|a(N_c);(0)_p,(0)_j\rangle$ and $|b(N_c);(0)_p,(0)_j\rangle$, which belong to two one-dimensional subspaces, are given by

$$G_{aa}(E_i+i\eta) = \frac{1}{E_i+i\eta-E_a-i\hbar\frac{W_{21}}{2}}, \tag{65a}$$

$$G_{bb}(E_i+i\eta) = \frac{1}{E_i+i\eta-E_b-i\hbar\frac{W_{31}+W_{32}}{2}}, \tag{65b}$$

where

$$E_a = 0, \tag{66a}$$

$$E_b = -\delta_c, \tag{66b}$$

$$E_i = \delta_p+\delta_c. \tag{66c}$$

Thus, the transition amplitude (Eq. 64) takes the form

$$\begin{aligned} T_{fi} &= \frac{\hbar\Omega}{2}\frac{1}{\hbar(\delta_p+i\gamma_{12})}\frac{\hbar\Omega_p}{2} + \\ & \frac{\hbar\Omega}{2}\frac{1}{\hbar\delta_c}\frac{\hbar\Omega_c}{2}\frac{1}{\hbar(\delta_p+\delta_c+i\gamma_{13})}\frac{\hbar\Omega_c}{2}\frac{1}{\hbar\delta_c}\frac{\hbar\Omega_p}{2}. \end{aligned} \tag{67}$$

The transition amplitude (Eq. 67) found here is the sum of two terms which are associated with two resonances. Figure 6 shows the two resonances in the dressed states picture.

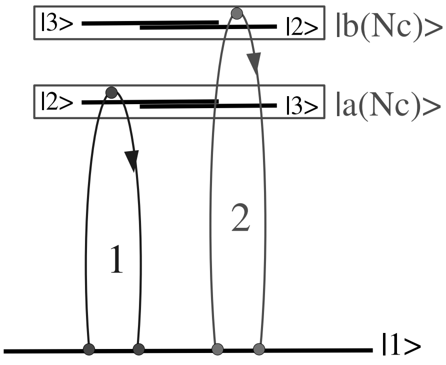

FIG. 6: Resonances of the Cascade-EIT configuration in the dressed states picture.

The first resonance corresponds to the excitation of the dressed atom from level $|1(N_c)\rangle$ to level $|a(N_c)\rangle$ followed by the decay to the ground state by spontaneous emission of one photon into the vacuum. The second term corresponds to a process which is very similar to the first but where the dressed atom gets excited to the dressed state $|b(N_c)\rangle$ not $|a(N_c)\rangle$.

The transition amplitude (Eq. 51), calculated in the bare states picture in the low saturation limit, has the same structure as the amplitude (Eq. 67) derived in the dressed states picture under the same conditions. The physical interpretations given for the two resonances, first resonance and second resonance, at the end of subsection IV B are consistent with the previous discussion given for the transition amplitude (Eq. 67). In this case, $\Omega_c^2/\delta_c^2 \ll 1$, the magnitude of the second resonance in equation 67 approaches the magnitude of the first resonance under the same condition $\Omega_c > \gamma_{13}$ which was introduced in the bare states picture.

C. Conclusions

In this section, Dressed States Picture, we clearly showed the physical difference between the Cascade-EIT and Cascade-AT configurations. In the weak coupling field regime, unlike the case in the Cascade-EIT setting where the scattering process of one probe photon can happen following either one of two distinct and compatible pathways, in the Cascade-AT setting only one evolution pathway dominates over the rest.

The existence of two scattering pathways of comparable probabilities in the Cascade-EIT configuration leads to the manifestation of interference effects. This remarkable interference phenomenon is absent in the Cascade-AT configuration where the atom follows only one scattering pathway in the low saturation limit.

VI. CONCLUSIONS

By applying the scattering technique we studied the Cascade-EIT configuration in the bare and dressed states pictures. The Cascade-AT configuration was studied only in the dressed states picture for reasons that were stated in section IV. In the Cascade-EIT case we showed that the transition amplitude is the sum of two complex numbers associated with two resonances. These resonances correspond to interfering scattering pathways which we described in the bare states picture (Fig. 4), and in the dressed states picture (Fig. 6) in the weak field regime. The transition amplitude corresponding to the Cascade-AT case was derived in the low saturation limit, and in the dressed states picture. The calculated amplitude was associated with one resonance presented in figure 5. The domination of only one scattering pathway eliminates the possibility of interference effects in the Cascade-AT configuration.

We also showed that after considering the low saturation limit, the derived transition amplitude (Eq. 51) for the Cascade-EIT configuration found in the bare states picture (Sec. V) approaches analytically the amplitude (Eq. 67) found in the Dressed states picture in the low saturation limit as well.

By studying the two cascade configurations, Cascade-EIT and Cascade-AT, we revealed two different coupling field regimes. We explored the weak field regime in detail and proved that unlike the AT effect EIT persists in the low saturation limit due to the existence of interference between competing pathways.

VII. ACKNOWLEDGMENTS

This work was conducted under the guidance and supervision of the late professor Lorenzo Narducci whom I dearly admire and miss. I would also like to thank Dr. Frank Narducci for critical reading of the manuscript and his genuine feedback.

[1] M. Fleischhauer, A. Imamoglu, and J. Marangos, Reviews of Modern Physics **77**, 633 (2005).

[2] E. Arimondo, *Progress in Optics* (North-Holland, 1996), vol. XXXV, chap. Coherent Population Trapping in Laser Spectroscopy, pp. 257–354.

[3] G. Grynberg, M. Pinard, and P. Mandel, Phys. Rev. A **54**, 776 (1996).

[4] S.E. Harris, J.E. Field, and A. Imamoglu, Phys. Rev. Lett. **64**, 1107 (1990).

[5] J. Marangos, J. Mod. Opt. **45**, 471 (1998).

[6] S. Harris, Phys. Today **50**, 36 (1997).

[7] K.-J. Boller, A. Imamoglu, and S.E. Harris, Phys. Rev. Lett. **66**, 2593 (1991).

[8] U. Fano, Phys. Rev. **124**, 1866 (1961).

[9] G. Alzetta, A. Gozzini, L. Moi, and G. Orriols, Nuovo Cimento B **36B**, 5 (1976).

[10] R. Whitley and J. Stroud, C.R., Phys. Rev. A **14**, 1498 (1976).

[11] E. Arimondo and G. Orriols, Lettere al Nuovo Cimento **17**, 333 (1976).

[12] H. Gray, R. Whitley, and J. Stroud, C.R., Optics Letters **3**, 218 (1978).

[13] S.E. Harris, J.E. Field, and A. Kasapi, Phys. Rev. A **46**, R29 (1992).

[14] M. Xiao, Y.-Q. Li, S.-Z. Jin, and J. Gea-Banacloche, Phys. Rev. Lett. **74**, 666 (1995).

[15] A. Kasapi, M. Jain, G.Y. Yin, and S.E. Harris, Phys. Rev. Lett. **74**, 2447 (1995).

[16] Z. D. L.V. Hau, S.E. Harris and C. Behroozi, Nature **397**, 594 (1999).

[17] M.M. Kash, V.A. Sautenkov, A.S. Zibrov, L. Hollberg, G.R. Welch, M.D. Lukin, Y. Rostovtsev, E.S. Fry, and M.O. Scully, Phys. Rev. Lett. **82**, 5229 (1999).

[18] A. M. Steinberg and R. Y. Chiao, Phys. Rev. A **49**, 3283 (1994).

[19] L. Wang, A. Kuzmich, and A. Dogariu, Nature **411**, 974 (2001).

[20] R. Boyd and D. J. Gauthier, *Progress in Optics* (Elsevier, Amsterdam, 2002), vol. 43, chap. 'Slow' and 'Fast' light, pp. 497–530.

[21] S. H. Autler and C. H. Townes, Phys. Rev. **100**, 703 (1955).

[22] C. Cohen-Tannoudji, *Amazing Light* (Springer, Berliln, 1996), chap. 11, pp. 109–123.

[23] J.E. Field, K.H. Hahn, and S.E. Harris, Phys. Rev. Lett. **67**, 3062 (1991).

[24] Y.Q. Li, S.Z. Jin, and M. Xiao, Phys. Rev. A **51**, R1754 (1995).

[25] J. Gea-Banacloche, Y.-Q. Li, S.-Z. Jin, and M. Xiao, Phys. Rev. A **51**, 576 (1995).

[26] J. Clarke, W. van Wijngaarden, and H. Chen, Phys. Rev. A **64**, 023818 (2001).

[27] B.K. Teo, D. Feldbaum, T. Cubel, J.R. Guest, P.R. Berman, and G. Raithel, Phys. Rev. A **68**, 53407 (2003).

[28] B. Lounis and C. Cohen-Tannoudji, J. Phys. II France **2**, 579 (1992).

[29] G. Grynberg and C. Cohen-Tannoudji, Opt. Commun. **96**, 150 (1993).

[30] G. Vemuri, G. Agarwal, and B. N. Rao, P.R.A. **53**, 2842 (1996).

[31] C. Cohen-Tannoudji and S. Reynaud, J. Phys. B **10**, 2311 (1977).

[32] C. Cohen-Tannoudji, J. Dupont-Roc, and G. Grynberg, *Atom-Photon Interactions: Basic Processes and Applications* (Wiley-Interscience, 1992).

[33] C. Cohen-Tannoudji and S. Haroche, J. Phys. (France) **30**, 153 (1969).